

A Snake-like Robot Incorporating Translational and Rotation Degrees of Freedom

Richard Primerano¹, Alexander Pietrocola¹ and Marco Janko¹

Abstract—Numerous snake-like robot mechanisms have been developed over the past several decades. A well studied kinematic structure consists of a series of segments coupled with rotational joints. In some designs, each segment is coupled with a 2-DOF joint. In others, segments are coupled through 1-DOF joints, with even numbered joints implementing yaw and odd numbered joints implementing pitch. In this paper, we present a robotic snake that implements both rotational and translational degrees of freedom in each joint. This new design allows for several new gaits to be implemented. We begin by presenting the mechanical design of the robot, and derive the kinematic equations of the robot's joints. Next, the electrical and communication systems are described. Finally, several gaits unique to this kinematic design are demonstrated.

I. INTRODUCTION

The unique construction of snake-like robots makes them well suited to many applications that are inappropriate for other types of mobile robots. Their small cross section allows them to access confined areas and their low center of mass allows them to maintain a stable footing on uneven terrains. This paper presents a new kinematic structure for snake-like robots that provides three degrees of freedom per segment, two of which are a translational degrees. One translational degree allows the robot to expand and contract along its length, producing a robot capable of “inchworm” type rectilinear motion. The other translational degree allows segments to offset laterally from one another. The third degree provides rotational motion between segments.

A. Organization

Section II provides a brief review of several well known snake-like robots and their kinematic structures. In Section III, we present the details of the mechanical design of our snake-like robot. The details of the electrical and software systems are given in Section IV. Several modes of locomotion are analyzed in Section V. Finally, concluding remarks are provided in Section VI.

II. BACKGROUND

Snake-like robots are classified in a variety of ways. Hirose groups snake-like robots into five classes based on joint kinematics (rotational vs. translational) and actuation (active vs. passive), as well as the presence of active wheels or treads [1]. Granosik distinguishes between *snake robots* and *serpentine robots* [2]. The former derive propulsion from joint motions only (no wheels, tracks, or legs) while the latter may use wheel, tracks or legs for propulsion. Since the introduction of Hirose's first robots, numerous variations on kinematic structure and propulsion method have been

examined in the literature. A small sampling of snake-like robot designs includes:

The ACM-R3 consists of a series of rigid links connected with rotational joints [3]. Joint orientations alternate between yaw and pitch. A passive wheel is located at each joint. This robot (as well as others in the ACM series) is well suited to achieve serpentine locomotion, and using this gait, it can move at high speeds. In addition, the robot can achieve several variations if lateral rolling.

The Unified Snake is kinematically similar to the ACM. It consists of a series of segments connected by 1-DOF joints, but relies only on body contact for locomotion as it possess no wheels [4]. The round cross section of this robot makes it well suited to execute the lateral rolling gait. The high strength of its actuators also allow for more complex gaits such as sidewinding and slithering [5].

The OmniTread consists of a series of segments connected by 2-DOF joints [2]. The outer surface of each segment is covered in a tank-like tread, allowing the robot to move over irregular surfaces easily. The design is unique in that a single drive motor provides power to all segments.

The ACM-S1 is kinematically similar to the ACM-R3, but adds an *elongation* motion between segments [6]. By allowing segments to expand and contract relative to one another, this robot can achieve an inchworm type motion in addition to the motions possible with the other ACM series robots. The inchworm motion is suited for applications where the robot must move through a confined environment where there is insufficient room to execute a rolling, slithering, or sidewinding gait.

III. MECHANICAL DESIGN

In this paper, we present a snake-like robot design where segments are connected to one another through a 3-DOF joint, each joint providing two translational degrees (including one for elongation) and one rotational degree. The assembled robot is shown in Figure 1. The snake shown here is ten segments long, though the modular design allows this length to be varied. Each segment is connected to its

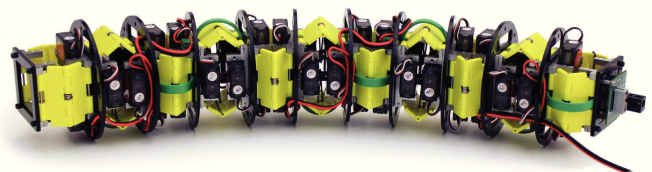


Fig. 1. The robotic snake consisting of ten segments.

neighbors with a pair of hinges and each hinged joint is actuated with four RC servo motors. The remainder of this section details the mechanical design of the robot, including the segment and overall robot kinematics.

A. Segment Kinematics

The snake is composed of a series of identical segments. Figure 2 shows the CAD model of one segment. The segment consists of a 4 in (201 mm) diameter ABS plastic rib, four RC servo motors, four ABS hinge leaves, a control circuit board, and four batteries. Note that batteries are omitted from the snake pictured in Figure 1.

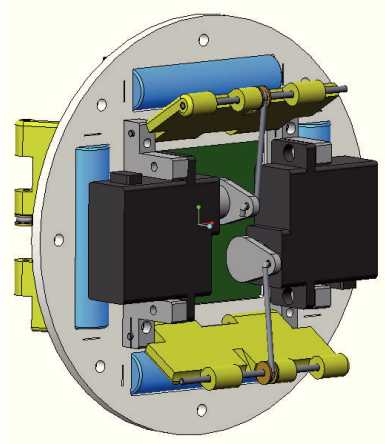


Fig. 2. CAD model of one segment of the snake

Figure 2 shows the front face of the segment. The hinge leaves are oriented horizontally and a connecting rod connects each hinge leaf to the horn of a servo. The rear of the segment is configured identically, except that all components are rotated 90°.

Close examination of the segment shows that the hinge leaf, connecting rod, and servo horn form three bars of a four bar linkage. Figure 3 shows two segments connected, forming a *joint* (several components have been hidden for

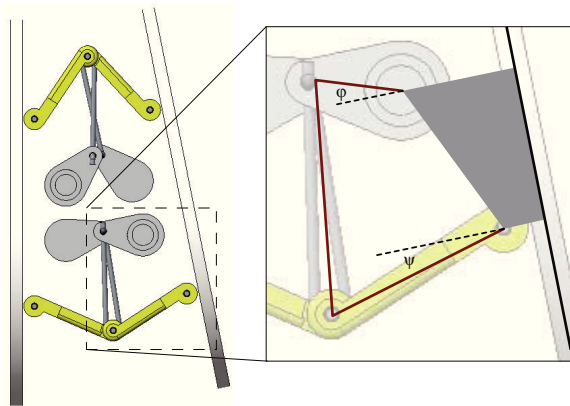


Fig. 3. The joint between segments is actuated through four 4-bar linkages

clarity). It also details the one of the four 4-bar linkages that actuate each joint.

The configuration of one segment with respect to its neighbor can be expressed with the triple $[x, y, \theta]$, shown in Figure 4. The segment *inverse kinematic* equations relate the position and orientation of a segment to the angles of the four servo motors ϕ_n driving that segment's joint. The inverse kinematics are calculated in two steps. First, the *hinge angles* ψ_n are calculated from the triple $[x, y, \theta]$ (once per hinge leaf), then a lookup table is used to determine the *servo horn angles* ϕ_n from the hinge angles ψ_n . A lookup table was chosen for this step to speed kinematic calculations in the robot's onboard processor, but the values can be calculated in real time.

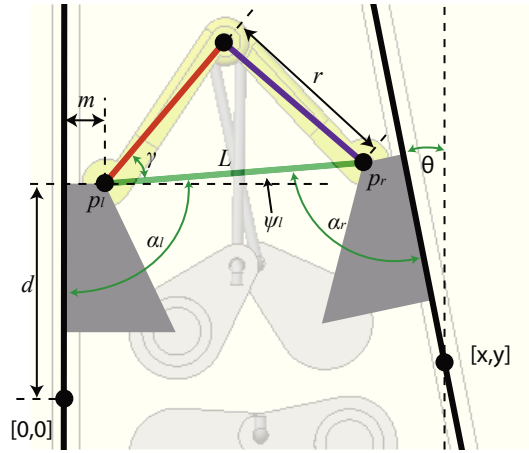


Fig. 4. Quantities used to derive the segment inverse kinematics

From Figure 4, given the desired joint configuration $[x, y, \theta]$, and the constants m , d , and r , the inverse kinematics of the segment are calculated by the following set of equations.

$$\begin{aligned} p_{lx} &= m \\ p_{ly} &= d \\ p_{rx} &= x + d \cdot \cos(\theta) + m \cdot \sin(\theta) \\ p_{ry} &= y + d \cdot \sin(\theta) - m \cdot \sin(\theta) \end{aligned}$$

$$\begin{aligned} L &= \|p_r - p_l\| \\ B &= p_{ry} - p_{ly} \\ H &= p_{rx} - p_{lx} \end{aligned}$$

$$\begin{aligned} \alpha_l &= (180/\pi) \cdot \text{atan}(H/B) \\ \alpha_r &= 180 - \theta - \alpha_l \\ \gamma &= (180/\pi) \cdot \text{acos}(L/(2r)) \end{aligned}$$

$$\begin{aligned} \psi_l &= \gamma + \alpha_l - 90 \\ \psi_r &= \gamma + \alpha_r - 90 \end{aligned}$$

Thus, we have derived an equation for the left and right

hinge leaf angles (ψ_l and ψ_r , respectively) in terms of the desired segment configuration $[x, y, \theta]$. This derivation gives the *upper* leaf angles since it was based in the kinematics of Figure 3. It can be verified that the same equation gives the *lower* leaf angles through the following relation,

$$[\psi_{ul} \ \psi_{ur}] = f(x, y, \theta) \quad (1)$$

$$[\psi_{ll} \ \psi_{lr}] = f(-x, y, -\theta) \quad (2)$$

where the first subscript of ψ denotes *lower* or *upper* leaf, and the second denotes *left* or *right* leaf. The final step is to relate the leaf angle to the servo horn angle, $\phi_n = g(\psi_n)$ (see Figure 3). This can be done in closed form, but we have implemented this with a lookup table to reduce processing burden. The inverse kinematic relation is extracted directly from the CAD package and used to build the lookup table. Figure 5 shows the relationship between hinge leaf angle ψ and servo motor angle ϕ .

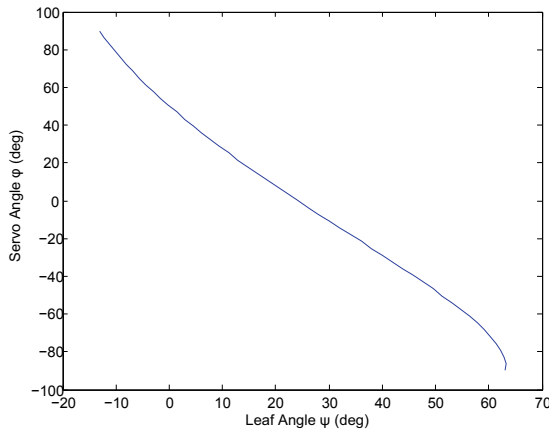


Fig. 5. The 4-bar linkage IK lookup table

The dual hinge mechanism that forms the joint provides three degrees of freedom demonstrated in Figure 6. The *bending* motion, shown in Figure 6(a), is one that is common to most snake-like robots. The *elongation* motion (Figures 6(b) and 6(c)) is seen in only a handful of snake-like robots, the ACM-S1 and Slim Slime [1] being two examples. The offset motion, shown in Figure 6(d), is, to the best of our knowledge, a new kinematic feature for snake-like robots. We will show in Section V that this motion contributes to several interesting gaits.

Joint Kinematic Constraints Note that the joint possesses *three* degrees of freedom while being actuated by *four* motors. The resulting kinematic structure is *overconstrained*, i.e. the four motor angles can not be independently varied. In order for the overconstrained structure to operate properly, all four motors must be controlled such that they simultaneously satisfy the joint constraints. A practical issue that arises with our design is that hobby RC servo motors suffer from part-to-part variation in their neutral position and full-scale rotation. To compensate, each motor must be trimmed prior to joint assembly. Neutral offset and full-scale gain values are stored in nonvolatile memory on each segment.

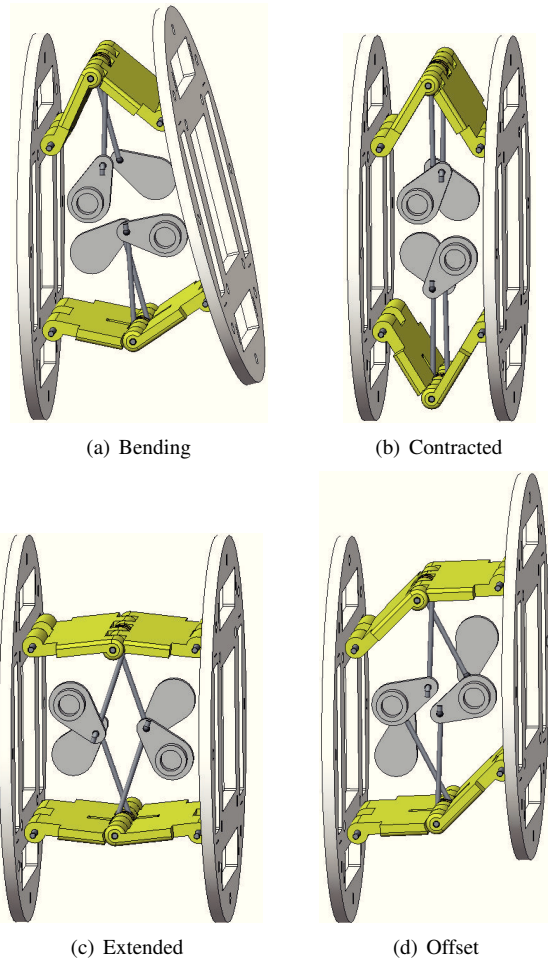


Fig. 6. Each joint provides three degrees of freedom.

If *any one* of the four motors is removed, the overconstrained joint becomes *fully constrained*. The three motor joint behaves identically to the original. We have chosen to include four motors in each joint, however, to increase overall joint force/torque.

B. Robot Kinematics

Each segment contains two “half-joints”. In Figure 2, we see one half-joint with its hinge leaves oriented horizontally, and there is an identical half joint on the back side with its hinges oriented vertically. The result of this structure is that if the first joint provides pitch and y-axis translation (two of its three degrees of freedom), the second joint provides yaw and x-axis translation. Both joints provide z-axis translation (elongation). An abstraction of a five joint snake’s kinematic structure is shown in Figure 7. The rectangular components

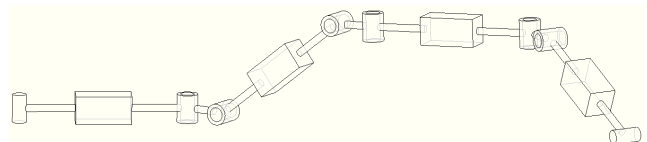


Fig. 7. A simplified representation of the robot (5 ribs, 4 joints)

represent *prismatic* joint and the cylindrical components represent *revolute* joints. Each snake joint can be considered a revolute-prismatic-revolute (RPR) chain and the snake's rib is a 90° coupler between RPR segments. The unique kinematics of this robot give rise to several interesting behaviors.

1) *Elongation*: The elongation behavior is shown in Figure 8. Using this characteristic, the robot can execute an inchworm-like rectilinear gait by alternately expanding and contracting segments.

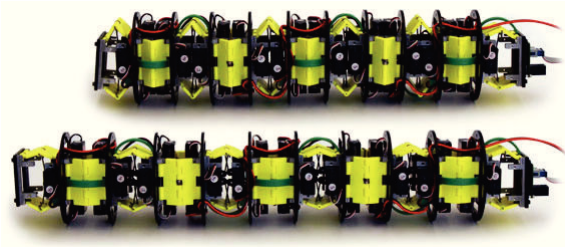


Fig. 8. Extension and contraction along the snake's body axis

2) *Spreading*: The robot has a round cross-section. While this makes the rolling gait easy to implement, it may pose a problem when executing rectilinear motion (where the robot's backbone curve is a line). The robot can increase its stability against rolling during such gaits by alternately shifting its segments in the manner shown in Figure 9.

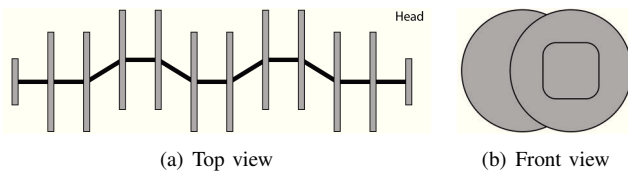


Fig. 9. The robot can offset its vertical segments to increase stability.

A summary of the snake's mechanical specifications is given in Table I.

TABLE I
MECHANICAL SPECIFICATION, 10 SEGMENT SNAKE

Parameter	Value
<i>General</i>	
Diameter	4 in (20.1 cm)
Length - robot	15 in to 20 in (38 cm to 51 cm)
Mass - robot	4.0 lb (1.8 kg)
Mass - segment	0.4 lb (0.18 kg)
<i>Rotational limits</i>	
Rotation	$\pm 20^\circ$
Torque	160 oz-in (1.13 N-m)
Speed (@ 80 oz-in load)	80^0 per sec
<i>Extension/Offset limits</i>	
Extension	0.5 in (1.25 cm)
Offset	± 0.75 in (1.90 cm)
Force	112 oz (3.2 N)
Speed (@ 48 oz load)	1 in/sec (2.54 cm/sec)

Note that the servo motors used here do not provide position feedback to the segment controller. The rotational and translational speed values given in Table I were measured with the joint loaded to 50% of their stall value.

IV. ELECTRICAL/SOFTWARE DESIGN

Each segment is controlled by its own processor. The segment circuit board, shown in Figure 10, contains the following features:

- Li-ion battery charge controller
- Battery and bus current monitoring
- CAN and UART board-to-board serial interfaces
- 6 V, 3 A switching regulator for servo power
- Expansion connector: SPI/I²C, analog in, digital I/O

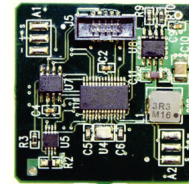


Fig. 10. The circuit board that controls the robot's segment

Each segment PCB has two ribbon cable connectors, the *upstream* connector faces the head of the snake and the *downstream* connector faces the tail. Each segment is connected to a CAN bus operating at 1 Mbps allowing peer-to-peer communication between segments. In addition, each segment has a dedicated 50kbps UART connection with its neighboring segments. The CAN bus is the primary communication channel, and the UART is used for address discovery and local communications. Figure 11 illustrates the communication architecture of the robot.

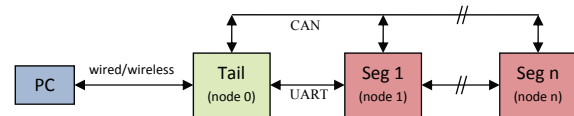


Fig. 11. The robot's communication architecture

In addition to the segment PCBs, a tail PCB acts as the bridge between the robot and a host controller. Messages enter the robot through the tail board. Depending on their destination address, the messages are either processed by the tail (address 0) or forwarded to the CAN bus to be processed by the appropriate segment. Likewise, messages on the CAN bus that are directed to address 0 are processed by the tail and those that are directed to the host controller (reserved address 250) are forwarded.

V. LOCOMOTION EXAMPLES

In this section, we present several gaits that our robot can use for locomotion. The translation degrees of freedom afforded by this design allow for unique variations on several well known gaits.

A. Lateral Rolling

The rolling gait has been studied and implemented by several groups [3], [5], [7], [8]. In this gait, a fixed *backbone curve* is defined and the snake is rotated about the curve. Most commonly, a C shaped curve is used, but V and S

curve rolling has also been demonstrated [3]. A simplified approximation to the C curve rolling gait can be obtained by driving the angular position of each joint with a sinusoidally varying setpoint as specified in 3.

$$\theta_n = \begin{cases} \alpha \cdot \sin(2\pi t/T) & : n \text{ odd} \\ \alpha \cdot \cos(2\pi t/T) & : n \text{ even} \end{cases} \quad (3)$$

where θ_n is the bending angle of the n^{th} segment, α is the maximum bending angle, and T is the period for one revolution of the robot.



Fig. 12. Overlay of three stages in the rolling gait

Figure 12 shows several overlaid images as the robot executes this maneuver. In this test, $\alpha = 10^\circ$ and $T = 2s$.

B. Offset Rolling

The joint kinematics of this robot allows for another type of rolling where the robot remains in a straight line and offsets its segments in an appropriate sequence. Figure 13 demonstrates six snapshots of this “offset rolling” gait.

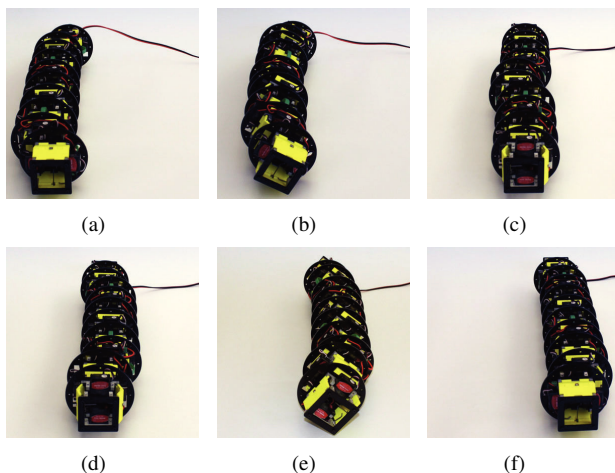


Fig. 13. Stages of the “offset rolling” gait - left to right, top to bottom

The following steps are depicted in the figure: (a) the robot begins by offsetting segments 1 and 10 to the right, (b) segments 5 and 6 are offset downward, tilting the robot 45° to the right, (c) segments 1 and 10 are retracted, causing the robot to continue rotating to 90° , (d) segments 5 and 6 are retracted while segments 3 and 7 are offset, (e) segments 1 and 10, now at a different orientation than they began, offset in the downward direction, rotating the robot an additional

45° , (f) finally, segments 3 and 7 retract, causing the robot to rotate to 180° .

C. Rectilinear Motion

Several snake-like robots can achieve a “near rectilinear” gait by producing a small amplitude vertically oriented sinusoidal ripple in the snake’s rotational joints. Several designs possess the extension mode needed for a true rectilinear motion, ACM-S1 and Slim Slime [1] being two examples. These robots locomote by alternately expanding and contracting their segments. The contact point between the robot and ground exhibits low friction when sliding forward but high friction in the reverse direction. The expansion/contraction cycle drags the robot forward. The concept is illustrated in our robot in Figure 14. Here, a “compression wave” propagates from the rear of the robot to the front. In this example, only one pair of joints is actuated at a time. As a result, one rib slides while the remaining nine ribs keep the robot anchored.

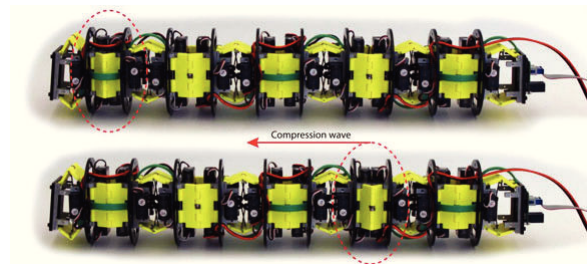


Fig. 14. A forward traveling compression wave carries the snake forward

A drawback of this type of rectilinear gait is that segments drag, leading to friction and energy use. Some work has been done toward the development of variable friction surfaces with the intent of improving the rectilinear gait [9]. The segment offset motion provided by our robot offers an alternative method of achieving improved rectilinear motion.

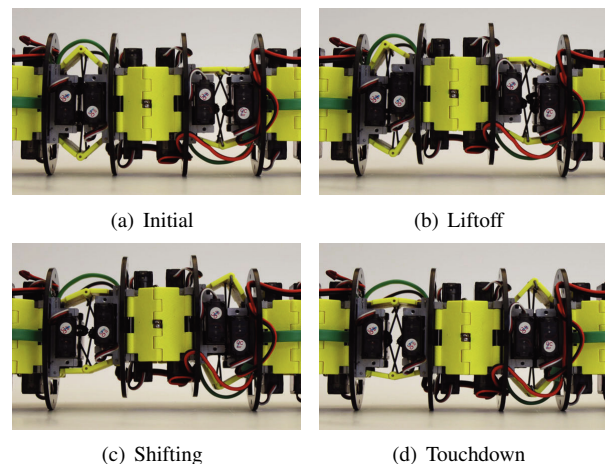


Fig. 15. Stages of the rectilinear gait - left to right, top to bottom

Figure 15 shows a close-up view of several segments of the snake while executing this alternate form of rectilinear

motion. Four ribs and three joints (*left*, *right*, and *middle*) are shown. The *middle* joint provides left-right offset and will remain locked during the maneuver. The left and right joints provide up-down offset and are active in the maneuver. The figure shows four stages in the motion cycle: (a) the left joint is contracted while the right is extended, neither joint is offset, (b) both joints offset, lifting the middle two ribs off the ground, (c) the middle ribs are shifted forward, and (d) the middle ribs are dropped back onto contact with the ground. After this cycle, the pair of ribs has been “carried” to the right. The process is repeated in sequence, one segment pair at a time, from tail to head. A benefit of this gait is that there is no sliding between the robot and surface.

VI. CONCLUSION

In this paper, we have introduced a new kinematic structure for snake-like robots. The design uses a dual hinge configuration to connect segments and provides three degrees of freedom per joint. Two of these degrees are translational, providing offset and extension, and allow the robot to achieve new forms of locomotion.

The next step in our research will be to characterize the performance of these new gaits as compared to existing ones, and better understand the relative strengths of these gaits in different operating environments.

REFERENCES

- [1] S. Hirose and H. Yamada, “Snake-like robots [tutorial],” *Robotics Automation Magazine, IEEE*, vol. 16, no. 1, pp. 88–98, March.
- [2] G. Granosik, M. G. Hansen, and J. Borenstein, “The omnitread serpentine robot for industrial inspection and surveillance,” *Industrial Robot: An International Journal*, vol. 32, no. 2, pp. 139–148, 2005.
- [3] M. Mori and S. Hirose, “Three-dimensional serpentine motion and lateral rolling by active cord mechanism acm-r3,” in *Intelligent Robots and Systems, 2002. IEEE/RSJ International Conference on*, vol. 1, pp. 829–834 vol.1.
- [4] C. Wright, A. Buchan, B. Brown, J. Geist, M. Schwerin, D. Rollinson, M. Tesch, and H. Choset, “Design and architecture of the unified modular snake robot,” in *Robotics and Automation (ICRA), 2012 IEEE International Conference on*, May, pp. 4347–4354.
- [5] F. Enner, D. Rollinson, and H. Choset, “Simplified motion modeling for snake robots,” in *Robotics and Automation (ICRA), 2012 IEEE International Conference on*, May, pp. 4216–4221.
- [6] S. Sugita, K. Ogami, M. Guarnieri, S. Hirose, and K. Takita, “a study on the mechanism and locomotion strategy for new snake-like robot active cord mechanismslime model 1 acm-s1,” *J. Robot. Mechatron*, vol. 20, no. 2, pp. 302–310, 2008.
- [7] G. Ford, R. Primerano, and M. Kam, “Crawling and rolling gaits for a coupled-mobility snake robot,” in *Advanced Robotics (ICAR), 2011 15th International Conference on*, 2011, pp. 556–562.
- [8] C. Ye, S. Ma, B. Li, H. Liu, and H. Wang, “Development of a 3d snake-like robot: Perambulator-ii,” in *Mechatronics and Automation, 2007. ICMA 2007. International Conference on*, Aug., pp. 117–122.
- [9] H. Marvi, J. Bridges, G. Meyers, G. Russell, and D. Hu, “Scalybot: a snake-inspired robot with active control of friction,” in *Proc. ASME Dynamic Systems and Control Conf., Arlington, VA, 31 October–2 November 2011*, 2011, pp. 443–450.